American Mineralogist, Volume 105, pages 239–243, 2020

Machiite, $Al_2Ti_3O_9$, a new oxide mineral from the Murchison carbonaceous chondrite: A new ultra-refractory phase from the solar nebula

Alexander N. Krot[1,*], Kazuhide Nagashima[1], and George R. Rossman[2]

[1]Hawai'i Institute of Geophysics and Planetology, University of Hawai'i at Mānoa, Honolulu, Hawai'i 96822, U.S.A.
[2]Division of Geological and Planetary Sciences, California Institute of Technology, Pasadena, California 91125, U.S.A.

Abstract

Machiite (IMA 2016-067), $Al_2Ti_3O_9$, is a new mineral that occurs as a single euhedral crystal, 4.4 μm in size, in contact with an euhedral corundum grain, 12 μm in size, in a matrix of the Murchison CM2 carbonaceous chondrite. The mean chemical composition of holotype machiite by electron probe microanalysis is (wt%) TiO_2 59.75, Al_2O_3 15.97, Sc_2O_3 10.29, ZrO_2 9.18, Y_2O_3 2.86, FeO 1.09, CaO 0.44, SiO_2 0.20, MgO 0.10, total 99.87, giving rise to an empirical formula (based on 9 oxygen atoms pfu) of $(Al_{1.17}Sc_{0.56}Y_{0.10}Ti^{4+}_{0.08}Fe_{0.06}Ca_{0.03}Mg_{0.01})(Ti^{4+}_{2.71}Zr_{0.28}Si_{0.01})O_9$. The general formula is $(Al,Sc)_2(Ti^{4+},Zr)_3O_9$. The end-member formula is $Al_2Ti_3O_9$. Machiite has the *C*2/*c* schreyerite-type structure with a = 17.10 Å, b = 5.03 Å, c = 7.06 Å, β = 107°, V = 581 Å^3, and Z = 4, as revealed by electron backscatter diffraction. The calculated density using the measured composition is 4.27 g/cm^3. The machiite crystal is highly ^{16}O-depleted relative to the coexisting corundum grain ($\Delta^{17}O$ = –0.2 ± 2.4‰ and –24.1 ± 2.6‰, respectively; where $\Delta^{17}O = \delta^{17}O - 0.52 \times \delta^{18}O$). Machiite is a new member of the schreyerite ($V_2Ti_3O_9$) group and a new Sc,Zr-rich ultrarefractory phase formed in the solar nebula, either by gas-solid condensation or as a result of crystallization from a Ca,Al-rich melt having solar-like oxygen isotopic composition ($\Delta^{17}O \sim -25$‰) under high-temperature (~1400–1500 °C) and low-pressure (~10^{-4}–10^{-5} bar) conditions in the CAI-forming region near the protosun. The currently observed disequilibrium oxygen isotopic composition between machiite and corundum may indicate that machiite subsequently experienced oxygen isotopic exchange with a planetary-like ^{16}O-poor gaseous reservoir either in the solar nebula or on the CM chondrite parent body. The name machiite is in honor of Chi Ma, mineralogist at California Institute of Technology, for his contributions to meteorite mineralogy and discovery of many new minerals representing extreme conditions of formation.

Keywords: Machiite, $Al_2Ti_3O_9$, $(Al,Sc)_2(Ti^{4+},Zr)_3O_9$, new mineral, Zr,Sc-rich phase, schreyerite group, ultrarefractory phase, Ca-Al-rich inclusion, Murchison meteorite, CM2 carbonaceous chondrite, oxygen isotopes

Introduction

During a mineralogical investigation of the Murchison meteorite, CM2 Mighei-type carbonaceous chondrite fell at Murchison, Victoria, Australia, on September 28, 1969, a new Zr,Sc-bearing, Al,Ti-oxide mineral, $(Al,Sc)_2(Ti^{4+},Zr)_3O_9$ with the *C*2/*c* schreyerite-type structure, named "machiite," was identified in the matrix (Figs. 1 and 2). To characterize its chemical and oxygen-isotope compositions, crystal structure, and associated phases, we used high-resolution scanning electron microscopy (SEM), electron backscatter diffraction (EBSD), electron probe microanalysis (EPMA), and secondary ion mass spectrometry (SIMS). Synthetic $Al_2Ti_3O_9$ was reported but not fully characterized (Colomban and Mazerolles 1991). Pang et al. (2018) identified vestaite, $(Ti^{4+},Fe^{2+},Al)_2Ti^{4+}_3O_9$ with minor $Al_2Ti_3O_9$ component, a new high-pressure mineral in eucrite NWA 8003. Presented here are the first natural occurrence of $Al_2Ti_3O_9$ in a primitive meteorite, as a new ultrarefractory mineral, and discussion of its origin and significance for nebular processes.

Mineral name and type material

The new mineral and its name have been approved by the Commission on New Minerals, Nomenclature and Classification of the International Mineralogical Association (IMA 2016-067) (Krot 2016). The mineral name is in honor of Chi Ma (born in 1968), mineralogist at California Institute of Technology, for his many contributions to meteorite mineralogy and discovery of 45 new minerals, including 14 refractory phases formed in the solar nebula and 11 high-pressure minerals resulted from shock metamorphism of meteorite parent bodies (e.g., Ma et al. 2014, 2015, 2016; Tschauner et al. 2014). Machiite is a new ultrarefractory phase, first observed by the first author (Alexander N. Krot) at University of Hawai'i, then identified as a new mineral by Ma and Krot using EBSD and EPMA at Caltech. The holotype specimen in Murchison section UH80 is in the Meteorite Collections at Hawai'i Institute of Geophysics and Planetology, University of Hawai'i at Mānoa, Honolulu, U.S.A.

Appearance, occurrence, and associated minerals

Machiite occurs as a single euhedral crystal, 4.4 μm in size, which is the holotype material, in contact (most likely in an intergrowth) with an euhedral 12 μm sized corundum grain in the fine-grained matrix of serpentine, tochilinite, and olivine in Murchison section UH80 (Fig. 1). The matrix is fine-grained, mainly containing serpentine, tochilinite, and olivine. Larger enstatite, olivine grains, and chondrules are scattered nearby in the matrix.

* E-mail: sasha@higp.hawaii.edu. Orcid 0000-0002-2278-8519.

0003-004X/20/0002–239$05.00/DOI: https://doi.org/10.2138/am-2020-7185

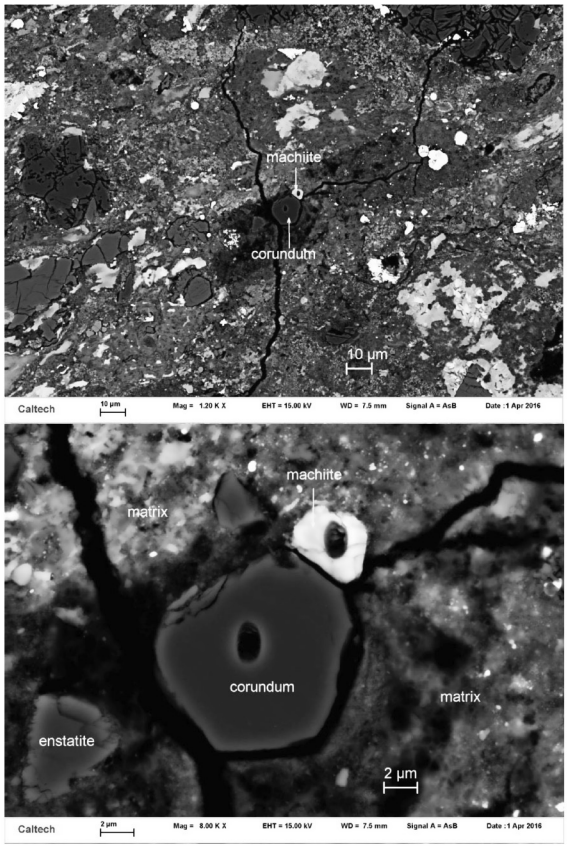

FIGURE 1. (**a**) Backscatter electron (BSE) image showing machiite in Murchison section UH80. (**b**) Enlarged BSE image showing the holotype machiite and associated corundum. The two holes are ion probe pits.

CHEMICAL AND OXYGEN ISOTOPIC COMPOSITIONS

Backscatter electron (BSE) images were obtained using a ZEISS 1550VP field emission SEM and a JEOL 8200 electron microprobe with solid-state BSE detectors. Six quantitative elemental microanalyses of holotype machiite were carried out using the JEOL 8200 electron microprobe operated at 10 kV (for a smaller interaction volume) and 5 nA in focused beam mode. Analyses were processed with the CITZAF correction procedure (Armstrong 1995) using the Probe for EPMA program from Probe Software, Inc. Analytical results are given in Table 1. The empirical formula (based on nine oxygen atoms pfu) of machiite is $(Al_{1.17}Sc_{0.56}Y_{0.10}Ti^{4+}_{0.08}Fe_{0.06}Ca_{0.03}Mg_{0.01})(Ti^{4+}_{2.71}Zr_{0.28}Si_{0.01})O_9$. The general formula is $(Al,Sc)_2(Ti^{4+},Zr)_3O_9$. The end-member formula is $Al_2Ti_3O_9$, which requires Al_2O_3 29.84, TiO_2 70.16, total 100.00 wt%. The corundum grain in contact with machiite contains Al_2O_3 99.52, TiO_2 0.68, FeO 0.65, total 100.84 wt%, having an empirical formula of $(Al_{1.98}Ti^{4+}_{0.01}Fe_{0.01})O_3$.

Oxygen isotopic compositions of machiite and corundum were measured in situ with the University of Hawai'i CAMECA ims-1280 SIMS using a primary Cs^+ ion beam accelerated to 10 keV and impacted the sample with an energy of 20 keV. A Cs^+ primary beam of ~20 pA focused to ~ 1–2 µm was used for pre-sputtering (180 s) and data collection (30 cycles of 20 s each). $^{16}O^-$, $^{17}O^-$, and $^{18}O^-$ were measured simultaneously using multicollection Faraday cup (FC), monocollection electron multiplier (EM), and multicollection EM, respectively. The mass resolving power on $^{16}O^-$ and $^{18}O^-$ was ~2000, while $^{17}O^-$ was measured with a mass resolving power of ~5500, sufficient to separate interfering $^{16}OH^-$. A normal incident electron flood gun was used for charge compensation. Data were corrected for FC background, EM deadtime, tail correction of $^{16}OH^-$, and instrumental mass fractionation (IMF). Because of the abundance sensitivity tail on the OH^- peak, we made a small tail correction (~0.2‰) on $^{17}O^-$ based on $^{16}OH^-$ count rate measured after each measurement. The IMF effects were corrected by standard-sample bracketing; for machiite and corundum using the Burma spinel standard. The reported 2σ uncertainties include both the internal measurement precision on an individual analysis and the external reproducibility for standard measurements. The external reproducibility of standard measurements (2 St.dev.) for both $\delta^{17}O$ and $\delta^{18}O$ was approximately ±2‰. Oxygen-isotope compositions, summarized in Table 2, are reported as $\delta^{17}O$ and $\delta^{18}O$, deviations from Vienna Standard Mean Ocean Water (VSMOW) in parts per thousand: $\delta^{17,18}O_{VSMOW} = [(^{17,18}O/^{16}O_{sample})/(^{17,18}O/^{16}O^{VSMOW}) - 1]\times 1000$, and as $\Delta^{17}O$ ($= \delta^{17}O - 0.52 \times \delta^{18}O$), deviation from the terrestrial fractionation (TF) line.

Machiite and corundum have distinctly different oxygen-isotope compositions with $\Delta^{17}O$ of –0.2 ± 2.4‰ and –24.1 ± 2.6‰, respectively (Table 2; Fig. 3). On a three-isotope oxygen diagram (Fig. 3a), compositions of machiite and corundum are displaced to the left and to the right from the Carbonaceous Chondrite Anhydrous Mineral (CCAM) line (Clayton et al. 1973, 1977) and Primitive Chondrule Mineral (PCM) line (Ushikubo et al. 2012) having approximately slope-1. The displacement of machiite could be a result of using a poorly matched standard (Burma spinel) for IMF corrections; in the case of corundum, mass-dependent fractionation during melt evaporation prior or during CAI crystallization cannot be excluded.

CRYSTALLOGRAPHY

Single-crystal electron backscatter diffraction (EBSD) analyses at a sub-micrometer scale were performed using an HKL EBSD system on a ZEISS 1550VP SEM, operated at 20 kV and 6 nA in focused beam mode with a 70° tilted stage and in a variable pressure mode (25 Pa) (Ma and Rossman 2008, 2009). The EBSD system was calibrated using a single-crystal silicon standard. The structure was determined and cell constants were obtained by matching the experimental EBSD patterns at different orientations with structures of Ti-oxides, Al_2TiO_5, and $V_2Ti_3O_9$ (schreyerite).

The EBSD patterns match the *C2/c* schreyerite $V_2Ti_3O_9$-type structure and give a best fit using the schreyerite cell from Döbelin et al. (2006) (Fig. 2), with a mean angular deviation of 0.64°, showing a = 17.10 Å, b = 5.03 Å, c = 7.06 Å, β = 107°, V = 581 Å^3, and Z = 4. The calculated density is 4.27 g/cm^3 using the empirical formula. Calculated X-ray powder diffraction data are given in Supplemental[1] Table S1. Micro-Raman analysis was attempted at Caltech with a Renishaw inVia Qontor Raman microscope using a green laser (514 nm) at 0.7 mW power in a confocal geometry. The collected Raman spectra showed broad features, likely derived from carbon and other materials trapped in the ion probe pit in the type crystal so that no distinct feature of machiite could be identified.

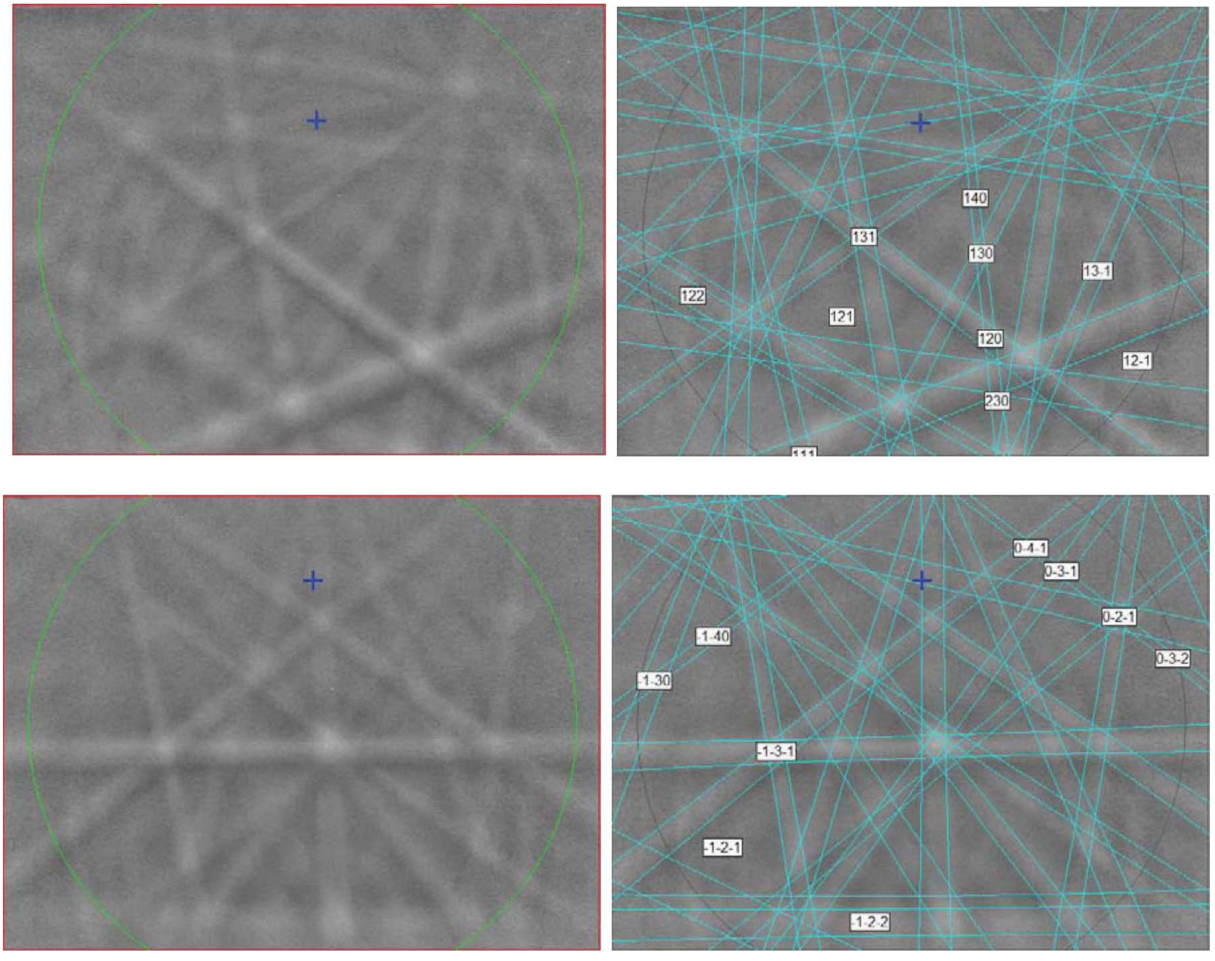

Figure 2. (**left**) EBSD patterns of the machiite crystal in Figure 1 at two different orientations, and (**right**) the patterns indexed with the *C*2/*c* $V_2Ti_3O_9$ structure. (Color online.)

Table 1. Average chemical composition of six point EPMA analyses for machiite

Constituent	wt%	Range	S.D.	Probe standard
TiO_2	59.75	58.49–60.49	0.72	TiO_2
Al_2O_3	15.97	15.61–16.24	0.25	anorthite
Sc_2O_3	10.29	10.03–10.64	0.21	$ScPO_4$
ZrO_2	9.18	8.56–9.88	0.44	Zircon
Y_2O_3	2.86	2.45–3.31	0.36	YPO_4
FeO	1.09	0.92–1.27	0.16	fayalite
CaO	0.44	0.41–0.49	0.03	anorthite
SiO_2	0.20	0.13–0.26	0.05	anorthite
MgO	0.10	0.04–0.18	0.05	forsterite
Total	99.87			

Table 2. Oxygen-isotope compositions of machiite and corundum in Murchison

Mineral	$\delta^{18}O$	2σ	$\delta^{17}O$	2σ	$\Delta^{17}O$	2σ
machiite	0.2	1.8	–0.1	2.2	–0.2	2.4
corundum	–35.3	1.6	–42.4	2.5	–24.1	2.6

Origin and significance

Machiite, $Al_2Ti_3O_9$, is a new member of the schreyerite group. It is the Al-analog of schreyerite $V_2Ti_3O_9$ and vestaite $(Ti^{4+}Fe^{2+})Ti_3^{4+}O_9$. Machiite contains high Zr and Sc (Table 1). Therefore, it is a new ultrarefractory phase, and it is among the first solids formed in the solar nebula.

The euhedral shape and texture of machiite with corundum in the Murchison matrix suggest its formation either by condensation or by crystallization from ultrarefractory melt. The ^{16}O-rich composition of corundum indicates that it crystallized in a ^{16}O-rich solar-like reservoir with $\Delta^{17}O$ of –24 ± 2‰. This value is similar to the oxygen-isotope composition of the sun inferred from the measurements of solar wind returned by the *Genesis* spacecraft ($\Delta^{17}O$ = –28.4 ± 3.6‰; McKeegan et al. 2011) and oxygen-isotope compositions of the majority of CAIs, including ultrarefractory inclusions from unmetamorphosed (petrologic types 2–3.0; Figs. 3a and 3b) chondrites (e.g., Makide et al. 2009; Ushikubo et al. 2012; Kööp et al. 2016; Krot et al. 2017a, 2017b, 2019; Komatsu et al. 2018), suggesting that the precursor material was probably an aggregate of refractory solids formed by condensation and/or evaporation in a gas of approximately solar composition in the CAI-forming region. Machiite, however, is in oxygen-isotope disequilibrium with the corundum and has nearly the terrestrial $\Delta^{17}O$ (~0‰). Isotopically heterogeneous (in respect to oxygen) ultrarefractory CAIs are commonly observed in metamorphosed CO (Figs. 3c and 3d) and CV chondrites

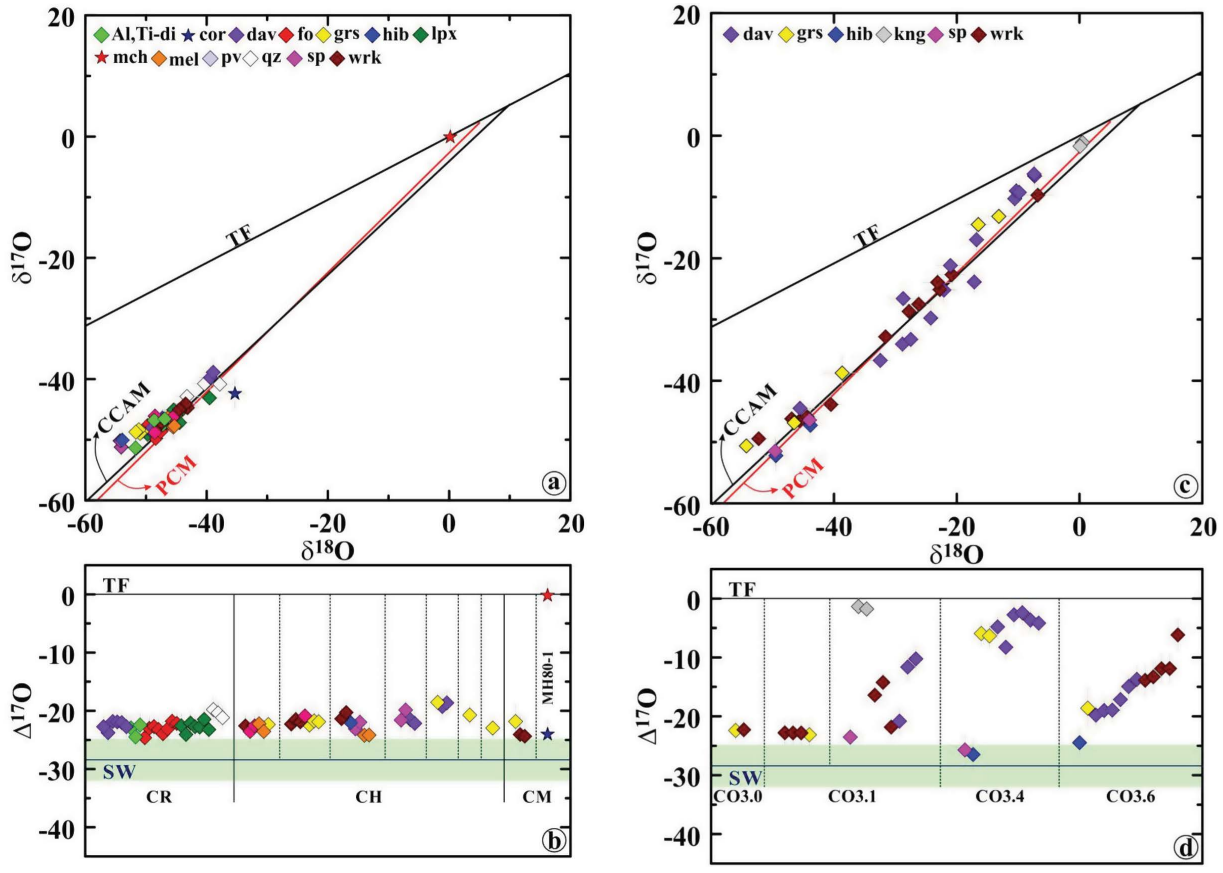

Figure 3. (**a** and **c**) Three-isotope oxygen diagrams and (**b** and **d**) $\Delta^{17}O$ of individual minerals of ultrarefractory CAIs from the (**a** and **b**) CR2, CH3.0, CM2, and (**c** and **d**) CO3.0–3.6 carbonaceous chondrites. In **b** and **d**, individual CAIs are separated by vertical lines. Most ultrarefractory CAIs from carbonaceous chondrites of petrologic type 2–3.0 have uniform oxygen isotopic compositions, except the machiite-corundum intergrowth MH80-1 from Murchison in which machiite is ^{16}O-depleted relative to corundum. Ultrarefractory CAIs from metamorphosed CO chondrites of petrologic types >3.0 have typically heterogeneous $\Delta^{17}O$: hibonite and spinel have low solar-like $\Delta^{17}O$; whereas warkite, kangite, and davisite are ^{16}O-depleted to various degrees. Al,Ti-di = Al,Ti-diopside; cor = corundum; dav = davisite; fo = forsterite; grs = grossite; hib = hibonite; kng = kangite; lpx = low-Ca pyroxene; mch = machiite; mel = melilite; pv = perovskite; qz = quarz; sp = spinel; wrk = warkite. CCAM = carbonaceous chondrite anhydrous mineral line (Clayton et al. 1973, 1977); PCM = primitive chondrule mineral line (Ushikubo et al. 2012); SW = solar wind returned by *Genesis* spacecraft (McKeegan et al. 2011); TF = terrestrial fractionation line. Data from Komatsu et al. (2018), Krot et al. (2019), and this study. (Color online.)

that experienced iron-alkali-halogen metasomatism (Brearley and Krot 2012). In the CV and CO ultratrefractory CAIs, Zr- and Sc-rich oxides and silicates, melilite, and perovskite are often ^{16}O-depleted relative to corundum, hibonite, spinel, Al-diopside, and forsterite (Krot et al. 2019). This mineralogically controlled oxygen-isotope heterogeneity is most likely due to post-crystallization isotope exchange with an ^{16}O-depleted external reservoir—either nebular gas (Yurimoto et al. 1998) or relatively high-temperature (>100 °C) aqueous fluid (Krot et al. 2019). Although CM chondrites appear to have experienced relatively low-temperature (20–70 °C) aqueous alteration (Guo and Eiler 2007), evidence for higher temperature alkali-halogen metasomatism, possibly driven by shock heating on the CM parent body, has been recently reported by Lee et al. (2019). Minor FeO concentrations in machiite (1.1 wt%) and associated corundum (0.7 wt%) imply some degree of Fe-metasomatism on the CM parent body. Due to the lack of knowledge of oxygen-isotope self-diffusion in machiite and other Zr- and Sc-rich minerals, the mechanism of oxygen-isotope exchange (gas-melt or gas-solid in the nebular or fluid-solid on the CM parent body) remains unclear.

Implications

Machiite is unique so far, identified only in Murchison. It most likely formed by condensation along with corundum or by crystallization from an ^{16}O-rich Ca, Al-rich melt under high-temperature (~1400–1500 °C) and low-pressure (~10^{-4}–10^{-5} bar) conditions in the CAI-forming region near the protoSun. Thermodynamic calculations show that at 10^{-4} bar total pressure, the condensation temperature of corundum and Zr is ~1400–1500 °C (Lodders 2003). Subsequently machiite experienced oxygen-isotope exchange with a ^{16}O-poor external reservoir, either nebular gas or aqueous fluid on the CM parent asteroid. Machiite is one of 15 newly approved refractory minerals discovered in

carbonaceous chondrites since 2007. Studies of these earliest solid materials are invaluable for understanding the details of nebular processes (evaporation, condensation, chemical, and isotopic fractionation) in the early solar system.

Acknowledgments and Funding

Comments and suggestions by J. Han, O. Tschauner, and anonymous reviewer are highly appreciated. SEM, EBSD, and EPMA were carried out at the Geological and Planetary Science Division Analytical Facility, Caltech, which is supported in part by NSF grants EAR-0318518 and DMR-0080065. SIMS was carried out at University of Hawai'i. Raman was carried out in the Rossman lab at Caltech. This work was also supported by NASA grant NNX17AE22G (P.I., A.N. Krot).

References cited

Armstrong, J.T. (1995) CITZAF: A package of correction programs for the quantitative electron beam X-ray analysis of thick polished materials, thin films, and particles. Microbeam Analysis, 4, 177–200.

Brearley, A.J., and Krot, A.N. (2012) Metasomatism in the early solar system: The record from chondritic meteorites. In D.E. Harlov and H. Austrheim, Eds., Metasomatism and the Chemical Transformation of Rock, Lecture Notes in Earth System Sciences, Springer, pp. 659–789.

Clayton, R.N., Grossman, L., and Mayeda, T.K. (1973) A component of primitive nuclear composition in carbonaceous chondrites. Science, 182, 482–485.

Clayton, R.N., Onuma, N., Grossman, L., and Mayeda, T.K. (1977) Distribution of the presolar component in Allende and other carbonaceous chondrites. Earth and Planetary Science Letters, 34, 209–224.

Colomban, P., and Mazerolles, L. (1991) Nanocomposites in mullite-ZrO_2 and mellite-TiO_2 systems synthesised through alkoxide hydrolysis gel routes: microstructure and fractography. Journal of Materials Science, 26, 3503–3510.

Döbelin, N., Reznitsky, L.Z., Sklyarov, E.V., Armbruster, T., and Medenbach, O. (2006) Schreyerite, $V_2Ti_3O_9$: New occurrence and crystal structure. American Mineralogist, 91, 196–202.

Guo, W., and Eiler, J.M. (2007) Temperatures of aqueous alteration and evidence for methane generation on the parent bodies of the CM chondrites. Geochimica et Cosmochimica Acta, 71, 5565–5575.

Komatsu, M., Fagan, T.J., Krot, A.N., Nagashima, K., Petaev, M.I., Kimura, M., and Yamaguchi, A. (2018) First evidence for silica condensation within the solar protoplanetary disk. Proceeding of National Academy of Sciences, 115, 7497–7502.

Kööp, L., Nakashima, D., Heck, P.R., Kita, N.T., Tenner, T.J., Krot, A.N., Nagashima, K., Park, C., and Davis, A.M. (2016) New constraints for the relationship between ^{26}Al and oxygen, calcium, and titanium isotopic variation in the early Solar System from a multi-element isotopic study of Spinel-Hibonite Inclusions. Geochimica et Cosmochimica Acta, 184, 151–172.

Krot, A.N. (2016) Machiite, IMA 2016-067. CNMNC Newsletter No. 34, December 2016, page 1317. Mineralogical Magazine, 80, 1315–1321.

Krot, A.N., Nagashima, K., Van Kooten, E.M.M., and Bizzarro, M. (2017a) High-temperature rims around calcium-aluminum-rich inclusions from the CR, CB and CH carbonaceous chondrites. Geochimica et Cosmochimica Acta, 201, 155–184.

——— (2017b) Calcium-aluminum-rich inclusions recycled during formation of porphyritic chondrules from CH carbonaceous chondrites. Geochimica et Cosmochimica Acta, 201, 185–223.

Krot, A.N., Ma, C., Nagashima, K., Davis, A.M., Beckett, J.R., Simon, S.B., Komatsu, M., Fagan, T.J., Brenker, F., Ivanova, M.A., and Bischoff, A. (2019) Mineralogy, petrography, and oxygen isotopic compositions of ultrarefractory inclusions from carbonaceous chondrites. Geochemistry, 79, 125519.

Lee, M.R., Cohen, B.E., and King, A.J. (2019) Alkali-halogen metasomatism of Meteorite Hills 01075 (CM2) driven by shock heating: An analogue for Ryugu. 82nd Annual Meeting of the Meteoritical Society, Abstract 6070.

Lodders, K. (2003) Solar system abundances and condensation temperatures of the elements. Astrophysical Journal, 591, 1220–1247.

Ma, C., and Rossman, G.R. (2008) Barioperovskite, $BaTiO_3$, a new mineral from the Benitoite Mine, California. American Mineralogist, 93, 154–157.

——— (2009) Tistarite, Ti_2O_3, a new refractory mineral from the Allende meteorite. American Mineralogist, 94, 841–844.

Ma, C., Beckett, J.R., and Rossman, G. (2014) Allendeite, ($Sc_4Zr_4O_{12}$), and hexamolybdenum (Mo,Ru,Fe), two new minerals from an ultrarefractory inclusion from the Allende meteorite. American Mineralogist, 99, 654–666.

Ma, C., Tschauner, O., Beckett, J.R., Liu, Y., Rossman, G.R., Zhuravlev, K., Prakapenka, V., Dera, P., and Taylor, L.A. (2015) Tissintite, (Ca,Na,□)$AlSi_2O_6$, a highly-defective, shock-induced, high-pressure clinopyroxene in the Tissint martian meteorite. Earth and Planetary Science Letters, 422, 194–205.

Ma, C., Tschauner, O., Becket, J.R., Liu, Y., Rossman, G.R., Sinogeikin, S.V., Smith, J.S., and Taylor, L.A. (2016) Ahrensite, γ-Fe_2SiO_4, a new shock-metamorphic mineral from the Tissint meteorite: implications for the Tissint shock event on Mars. Geochimica et Cosmochimica Acta, 184, 240–256.

Makide, K., Nagashima, K., Krot, A.N., Huss, G.R., Hutcheon, I.D., and Bischoff, A. (2009) Oxygen- and magnesium-isotope compositions of calcium-aluminum-rich inclusions from CR2 carbonaceous chondrites. Geochimica et Cosmochimica Acta, 73, 5018–5051.

Makide, K., Nagashima, K., Krot, A.N., Huss, G.R., Hutcheon, I.D., Hellebrand, E., and Petaev, M.I. (2013) Heterogeneous Distribution of ^{26}Al at the Birth of the Solar System: Evidence from Corundum-bearing Refractory Inclusions in Carbonaceous Chondrites. Geochimica et Cosmochimica Acta, 110, 190–215.

McKeegan, K.D., Kallio, A.P.A., Heber, V.S., Jarzebinski, G., Mao, P.H., Coath, C.D., Kunihiro, T., Wiens, R.C., Nordholt, J.E., Moses, R.W. Jr., and others. (2011) The oxygen isotopic composition of the Sun inferred from captured solar wind. Science, 332, 1528–1532.

Pang, R.-L., Harries, D., Pollok, K., Zhang, A.-C., and Langenhorst, F. (2018) Vestaite, ($Ti^{4+}Fe^{2+}$)$Ti^{4+}_3O_9$, a new mineral in the shocked eucrite Northwest Africa 8003. American Mineralogist, 103, 1502–1511.

Tschauner, O., Ma, C., Beckett, J.R., Prescher, C., Prakapenka, V.B., and Rossman, G.R. (2014) Discovery of bridgmannite, the most abundant mineral in Earth, in a shocked meteorite. Science, 346, 1100–1102.

Ushikubo, T., Kimura, M., Kita, N.T., and Valley, J.W. (2012) Primordial oxygen isotope reservoirs of the solar nebula recorded in chondrules in Acfer 094 carbonaceous chondrite. Geochimica et Cosmochimica Acta, 90, 242–264.

Yurimoto, H., Ito, M., and Nagasawa, H. (1998) Oxygen isotope exchange between refractory inclusion in Allende and solar nebula gas. Science, 282, 1874–1877.

Manuscript received June 28, 2019
Manuscript accepted September 25, 2019
Manuscript handled by Oliver Tschauner

Endnote:

[1]Deposit item AM-20-27185, Supplemental Material. Deposit items are free to all readers and found on the MSA website, via the specific issue's Table of Contents (go to http://www.minsocam.org/MSA/AmMin/TOC/2020/Feb2020_data/Feb2020_data.html).